

Real-time Closed Loop Neural Decoding on a Neuromorphic chip

Shoeb Shaikh¹, Rosa So², Tafadzwa Sibindi³, Camilo Libedinsky³ and Arindam Basu¹

Abstract—This paper presents for the first time a real-time closed loop neuromorphic decoder chip-driven intra-cortical brain machine interface (iBMI) in a non-human primate (NHP) based experimental setup. Decoded results show trial success rates and mean times to target comparable to those obtained by hand-controlled joystick. Neural control trial success rates of $\approx 96\%$ of those obtained by hand-controlled joystick have been demonstrated. Also, neural control has shown mean target reach speeds of $\approx 85\%$ of those obtained by hand-controlled joystick. These results pave the way for fast and accurate, fully implantable neuromorphic neural decoders in iBMIs.

I. INTRODUCTION

Intra-cortical Brain Machine Interfaces (iBMIs) have made it possible for patients suffering from paralysis to establish communication, locomotion [2] and even perform complex tasks such as feeding oneself [3], [4] solely through neural control. It is indeed heartwarming to see these chronic patients take a step towards leading normal lives as seen in demo videos presented in [3] and [4].

iBMI systems can be typically broken down into the following blocks a) Signal acquisition and pre-processing, b) Feature extraction, c) Decoding and d) Effector. The signal acquisition block consists of a microelectrode array sampling extracellular neuronal electrical activity at around 30 - 40 kHz. This recorded activity data is conventionally passed on through wires/cables to bulky signal processing systems implementing blocks b), c) and d). These wires/cables leave an opening in the skull making the area prone to infection. They also impede the mobility of the system as a whole. To tackle the mobility issue, solutions such as [5]–[11] with wireless transmitter electronics outside the skin have been reported. However, these still have the presence of infection-prone transcutaneous wires. Meanwhile, mobile fully implantable and hermetically sealed prototypes with decreased risk of infection have been reported in [12]–[14]. However, with exponentially rising number of electrodes [15], [16] and the concomitant increase in data rates, it is untenable to scale the idea of transmitting raw data in a fully implantable manner without heating up neural tissue excessively [17], [18] or hitting bandwidth constraints [19].

In order to solve this problem, we present a system level design space exploration in section II and advocate for performing operations up to decoding in the implant

itself. There have been suggestions made along similar lines in the works reported in [20]–[24]. However, [22]–[24] have reported offline results on pre-recorded data, of which [23] has only implemented the proof of concept on an FPGA thus not presenting true energy benefits and also not showing live experimental results. [21] has reported a real-time demonstration but the experiment has been performed on an anesthetized rat instead of the more standard use of awake non-human primates (NHP) and benchmarking has not been provided against state of the art decoding techniques. Authors in [20] have done an extensive study on standard experimental protocol of two NHPs in real-time. They have also benchmarked their algorithm against state of the art decoding technique, but the proposed decoder has been implemented in software leaving room for hardware demonstration.

We present for the first time a real-time closed loop demonstration of a fully brain controlled neuromorphic decoder chip in an experimental setup involving an NHP. Previously, offline results comparing this decoder chip with state of the art technique were reported in [25] in a similar experimental setup. We have benchmarked real-time brain controlled neuromorphic decoder's performance against hand-controlled joystick following the paradigm reported in [26].

II. iBMI's - A SYSTEM LEVEL REVIEW

The state of the art iBMI systems can be illustrated in Fig. 1.

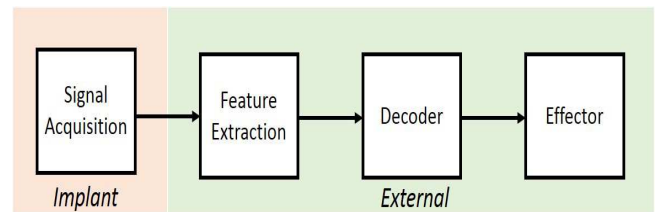


Fig. 1. Typical block diagram of an iBMI system

If we consider a typical case of a 100 electrode array with a sampling rate of 20 kHz and raw data digitized at 12 bits, the transmission rate becomes 24 Mbps. A fully implantable solution reported for this transmission rate yields ≈ 7 hours of continuous operation powered by a rechargeable Li-ion battery [13]. Reported time for charging the battery is two hours, which makes daily use quite cumbersome and impractical. To eliminate this frequent recharging owed principally to the broadband data rate [27], we propose incorporating the feature extraction and decoding blocks in the implant itself.

*This work was supported through grant RG87/16 by MOE, Singapore
¹Authors are with Nanyang Technological University, Singapore
 arindam.basu@ntu.edu.sg

²Author is with the Institute for Infocomm Research, Singapore
 rosa-so@i2r.a-star.edu.sg

³Authors are with SiNAPSE, National University of Singapore, Singapore
 camilo@nus.edu.sg

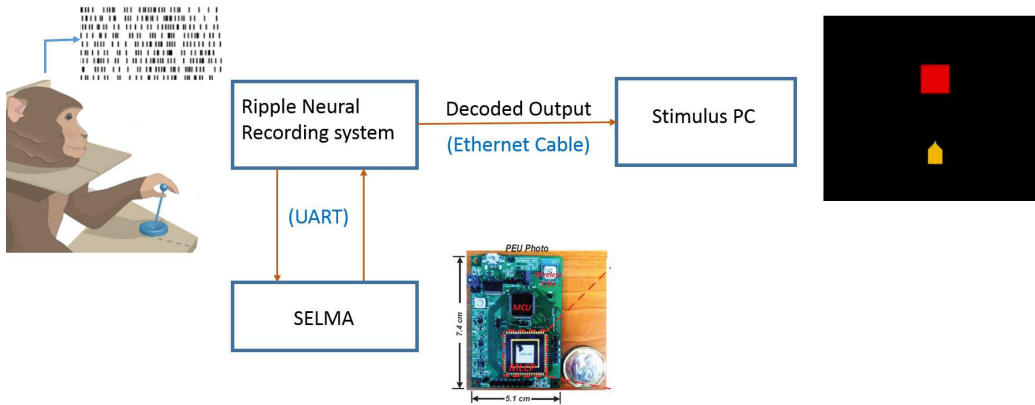


Fig. 4. Experimental setup for closed loop decoding with SELMA. SELMA and NHP figures are adapted from [24] and [30] respectively.

The decoder takes spikes as inputs as they occur at the respective electrodes. The input processing circuit then computes the average firing rate for every channel based on a user defined time bin of T_w seconds and updates it every T_s seconds. This is followed by the current mirror array which exploits the inherent mismatch of transistors to implement the first layer of ELM in a power and area-efficient manner. The hidden nodes are implemented in the form of current controlled oscillators, which integrate the summed currents and yield an output every T_s seconds. The hidden layer outputs are then multiplied by the weights stored in TI-MSP430 to yield the decoded outputs every T_s seconds.

IV. METHODS

A. Neural Signal Acquisition and Signal Processing

Two floating microwire arrays (32 electrodes each) were implanted in an NHP (*Macaca fascicularis*) in the left primary motor cortex area. Ripple’s grapevine neural recording system [31] was used for real-time recording of raw neural data sampled at 30 kHz. Spikes were detected using median absolute deviation method [32] with the threshold set as negative of five times the median.

B. Behavioural Task

An NHP is trained to maneuver a joystick using his left hand to drive a virtual wheelchair avatar towards a square target appearing on a computer screen in the hand-controlled joystick mode. In a given trial, wheelchair avatar starts at the centre of the screen and the target is presented in a pseudo-random manner in one of the three different directions – Forward, right and left in the form of a square of side 2 cm. The wheelchair avatar is driven in a discrete control fashion at a frequency of 10 Hz with possible position updates being one of left, right, forward or stop depending on the position of the joystick. A trial is considered successful if the NHP reaches, and stays in the target area for 1.5 seconds under a total elapsed time of 13 seconds. Once the NHP was trained well enough to perform the trials consistently, we proceeded to the neural control mode wherein the joystick is removed and the avatar is driven by the decoded outputs at 10 Hz. It

has been observed that in the absence of joystick, the NHP makes little or no overt movements.

C. Decoder Training

The decoder was trained on a total of three sessions consisting of 20 trials each. The NHP was made to passively observe a series of successful trials for the first couple of sessions following the training paradigm in [26]. Thereafter, an intermediate model M_{int} was trained based on these sessions. In the third session, M_{int} was employed with 50% assistance [30], [33] in the system and the final trained model M_f was obtained including data from all three sessions. Only successful trials were used for training the model.

V. RESULTS

The trained model M_f was tested until the NHP performed 60 successful trials each day by neural control. This experiment requires at least $\approx 70\%$ [30] of the decoded directions to match ground truth for a trial to be successful.

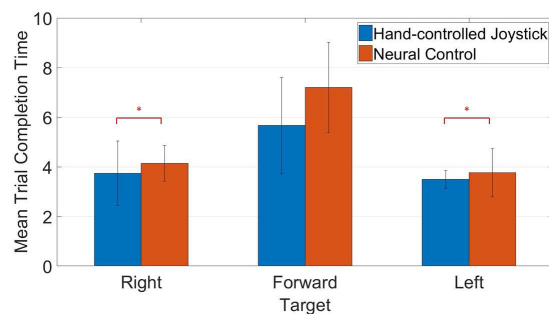


Fig. 5. Mean times to complete trials are comparable for closed-loop decoding by SELMA and hand controlled joystick experiments. Statistically insignificant difference is denoted by (*), $p > 0.01$ (unpaired two-sample t-test)

Chance level accuracy for the trained classifier model is 25%, so the chance level of success of a trial can be computed as $0.25^{(0.7 \times 130)} \times 100 \approx 0\%$. Closed-loop decoding results are benchmarked against those obtained from hand-controlled joystick experiments. We have compared a total of 180 hand-controlled joystick and neural decoder controlled

closed loop trials over a period of 3 days with 60 trials performed on each day.

Mean successful trial completion speeds for forward, left and right targets by brain control have been shown to be $\approx 79\%$, 93% and 90% respectively of those obtained by hand-controlled joystick. The results are plotted in Fig. 5.

Mean success rates for closed-loop brain control is $\approx 96\%$ of that obtained by hand-joystick control as shown in Fig. 6.

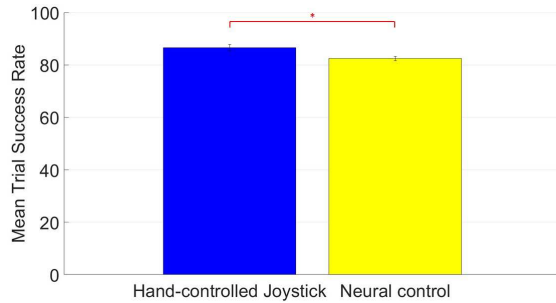


Fig. 6. Percentage of successful trials for hand-controlled joystick and neural control. Statistically insignificant difference is denoted by (*), $p > 0.01$ (unpaired two-sample t-test)

VI. CONCLUSION

From infection mitigation and mobility standpoints, a fully implantable iBMI is the one plausible approach. Neuromorphically engineered iBMI systems have long been touted as a viable option, albeit without hardware-based demonstration in standard NHP based experimental setups. We have demonstrated for the first time fast and accurate neural control obtained via a neuromorphic chip decoder in a closed loop NHP based experimental setup. The decoding accuracies are similar to those obtained in hand-controlled joystick experiments paving the way for future implanted system development.

ACKNOWLEDGMENT

The authors would like to thank Abdur Rauf for helping in animal training and data collection.

REFERENCES

- [1] Pandarinath, *et al.*, “High performance communication by people with paralysis using an intracortical brain-computer interface,” *eLife*, p. e18554, 2017.
- [2] Rajangam, *et al.*, “Wireless cortical brain-machine interface for whole-body navigation in primates,” vol. 6, 03 2016.
- [3] Collinger, *et al.*, “High-performance neuroprosthetic control by an individual with tetraplegia,” *Lancet (London, England)*, no. 9866, pp. 557–64, 2013.
- [4] Ajiboye, *et al.*, “Restoration of reaching and grasping movements through brain-controlled muscle stimulation in a person with tetraplegia: a proof-of-concept demonstration,” *The Lancet*, no. 10081, pp. 1821–1830, 2017.
- [5] Gao, *et al.*, “HermesE: A 96-Channel Full Data Rate Direct Neural Interface in $0.13 \mu\text{m}$ CMOS,” *IEEE Journal of Solid-State Circuits*, no. 4, pp. 1043–1055, 2012.
- [6] Miranda, *et al.*, “HermesD: A high-rate long-range wireless transmission system for simultaneous multichannel neural recording applications,” *IEEE Transactions on Biomedical Circuits and Systems*, vol. 4, no. 3, pp. 181–191, 2010.

- [7] Chestek, *et al.*, “HermesC: Low-power wireless neural recording system for freely moving primates,” *IEEE Transactions on Neural Systems and Rehabilitation Engineering*, vol. 17, no. 4, pp. 330–338, Aug 2009.
- [8] Santhanam, *et al.*, “HermesB: A continuous neural recording system for freely behaving primates,” *IEEE Transactions on Biomedical Engineering*, vol. 54, no. 11, pp. 2037–2050, 2007.
- [9] Ming Yin, *et al.*, “A 100-Channel Hermetically Sealed Implantable Device for Chronic Wireless Neurosensing Applications,” *IEEE Transactions on Biomedical Circuits and Systems*, no. 2, pp. 115–128, 2013.
- [10] Zanos, *et al.*, “The neurochip-2: An autonomous head-fixed computer for recording and stimulating in freely behaving monkeys,” *IEEE Transactions on Neural Systems and Rehabilitation Engineering*, vol. 19, no. 4, pp. 427–435, 2011.
- [11] Schwarz, *et al.*, “Chronic, wireless recordings of large-scale brain activity in freely moving rhesus monkeys,” *Nature Methods*, no. 6, pp. 670–676, 2014.
- [12] Rizk, *et al.*, “A fully implantable 96-channel neural data acquisition system,” *Journal of neural engineering*, vol. 6, no. 2, p. 026002, 2009.
- [13] Borton, *et al.*, “An implantable wireless neural interface for recording cortical circuit dynamics in moving primates,” *Journal of Neural Engineering*, vol. 10, no. 2, 2013.
- [14] Harrison, *et al.*, “A low-power integrated circuit for a wireless 100-electrode neural recording system,” *IEEE Journal of Solid-State Circuits*, vol. 42, no. 1, pp. 123–133, 2007.
- [15] Stevenson *et al.*, “How advances in neural recording affect data analysis,” *Nature neuroscience*, no. 2, pp. 139–42, 2011.
- [16] Jun, *et al.*, “Fully integrated silicon probes for high-density recording of neural activity,” *Nature*, no. 7679, pp. 232–236, Nov.
- [17] Kim, *et al.*, “Thermal impact of an active 3-D microelectrode array implanted in the brain,” *IEEE Transactions on Neural Systems and Rehabilitation Engineering*, vol. 15, no. 4, pp. 493–501, 2007.
- [18] Dethier, *et al.*, “Spiking neural network decoder for brain-machine interfaces,” in *2011 5th International IEEE/EMBS Conference on Neural Engineering*, April 2011, pp. 396–399.
- [19] S. Mohammed *et al.*, “Enabling Advanced Inference on Sensor Nodes Through Direct Use of Compressively-sensed Signals,” *Proceedings of the Design Automation and Test in Europe (DATE)*, 2012.
- [20] Dethier *et al.*, “Design and validation of a real-time spiking-neural-network decoder for brain-machine interfaces,” *Journal of Neural Engineering*, vol. 10, no. 3, p. 036008, 2013.
- [21] Boi, *et al.*, “A Bidirectional Brain-Machine Interface Featuring a Neuromorphic Hardware Decoder,” *Frontiers in Neuroscience*, no. December, pp. 1–15, 2016.
- [22] Jiang, *et al.*, “Microwatt end-to-End digital neural signal processing systems for motor intention decoding,” *Proceedings of the 2017 Design, Automation and Test in Europe, DATE 2017*, pp. 1008–1013, 2017.
- [23] Rapoport, *et al.*, “Efficient Universal Computing Architectures for Decoding Neural Activity,” *PLoS ONE*, vol. 7, no. 9, 2012.
- [24] Chen, *et al.*, “A 128-Channel Extreme Learning Machine-Based Neural Decoder for Brain Machine Interfaces,” *IEEE Transactions on Biomedical Circuits and Systems*, vol. 10, no. 3, pp. 679–692, 2016.
- [25] Shaikh, *et al.*, “Cortical motor intention decoding on an analog co-processor with fast training for non-stationary data,” in *2017 IEEE Biomedical Circuits and Systems Conference (BioCAS)*. IEEE, Oct., pp. 1–4.
- [26] Gilja, *et al.*, “A high-performance neural prosthesis enabled by control algorithm design,” *Nature Neuroscience*, vol. 15, no. 12, pp. 1752–1757, 2012.
- [27] Harrison, “The Design of Integrated Circuits to Observe Brain Activity,” *Proceedings of the IEEE*, vol. 96, no. 7, pp. 1203–1216, 2008.
- [28] Huang *et al.*, “Extreme learning machine for regression and multiclass classification,” *IEEE transactions on systems, man, and cybernetics. Part B, Cybernetics*, no. 2, pp. 513–29, 2012.
- [29] Huang, *et al.*, “Extreme learning machine: Theory and applications,” *Neurocomputing*, vol. 70, no. 1-3, pp. 489–501, 2006.
- [30] Libedinsky, *et al.*, “Independent mobility achieved through a wireless brain-machine interface,” *PLoS ONE*, vol. 11, no. 11, pp. 1–13, 2016.
- [31] “Ripple Neuro.” [Online]. Available: <http://rippleneck.com/>
- [32] Quiroga, *et al.*, “Unsupervised Spike Detection and Sorting with Wavelets and Superparamagnetic Clustering,” *Neural Computation*, no. 8, pp. 1661–1687.
- [33] Sadtler, “Investigating the Neural Basis of Learning Using Brain-Computer Interfaces,” 2014.